On the inward drift of runaway electrons in plateau regime

Di Hu[1, a)] and Hong Qin[2, 3]

[1)] *School of Physics, Peking University, Beijing 100871, China.*

[2)] *Princeton Plasma Physics Laboratory, Princeton University, Princeton, New Jersey, 08540, USA*

[3)] *School of Nuclear Science and Technology and Department of Modern Physics, University of Science and Technology of China, Hefei, 230026, China.*

(Dated: 6 January 2016)

The well observed inward drift of current carrying runaway electrons during runaway plateau regime after disruption is studied by considering the phase space dynamic of runaways in a large aspect ratio toroidal system. We consider the case where the toroidal field is unperturbed and the toroidal symmetry of the system is preserved. The invariance of canonical angular momentum in such system requires runaways to drift horizontally in configuration space for any given change in momentum space. The dynamic of this drift can be obtained by taking the variation of canonical angular momentum. It is then found that runaway electrons will always drift inward as long as they are decelerating. This drift motion is essentially non-linear, since the current is carried by runaways themselves, and any runaway drift relative to the magnetic axis will cause further displacement of the axis itself. A simplified analytical model is constructed to describe such inward drift both in ideal wall case and no wall case, and the runaway current center displacement as a function of parallel momentum variation is obtained. The time scale of such displacement is estimated by considering effective radiation drag, which shows reasonable agreement with observed displacement time scale. This indicates that the phase space dynamic studied here plays a major role in the horizontal displacement of runaway electrons during plateau regime.

PACS numbers: 45.20.Jj & 52.20.Dq

[a)] While visiting at PPPL, Princeton, New Jersey; Electronic mail: hudi_2@pku.edu.cn

I. INTRODUCTION

Large quantity of relativistic runaway electrons is one of the most feared by-product of tokamak disruption, especially for large devices with higher total plasma current and higher poloidal magnetic flux[1]. Those highly relativistic electrons are the direct result of high toroidal inductive field during disruption, which in turn is the consequence of drastically arising bulk plasma resistivity as the thermal energy is mostly lost after thermal quench[2,3]. If left unchecked, runaway electrons can multiply exponentially by Coulomb-collision avalanche[1], and up to 70% of initial plasma current can be converted into relativistic runaway current, forming the so called "runaway current plateau"[4]. Furthermore, the high energy electrons will keep being accelerated until effective radiation drag from synchrotron radiation and bremsstrahlung radiation finally balance the toroidal inductive field[5–7]. This will result in a highly anisotropic relativistic electron beam with energy on the order of tens of MeVs[8], as well as a "bump on the tail" kind of distribution function in the momentum-space[9–11].

The evolution of runaway electrons in momentum-space has been under substantial investigation during past decades[5–7,12–14]. However, the corresponding evolution in configuration space has not received due attention. During the aforementioned runaway current plateau, it is widely observed that there is a gradual inward drift of runaway current[15–17]. This inward drift will ultimately result in the intersection between runaway electrons and the wall, causing tremendous damage to the first wall due to its localized way of energy deposition[18]. The reason of this displacement is attributed to the force imbalance under externally generated vertical field[16], while the possible role played by the dynamic of relativistic electrons in a self-generated magnetic field has not been fully explored.

Similar horizontal drift of runaway orbit has been studied using test particle model[19]. It is found that the conservation of canonical angular momentum of runaway electrons will induce a trajectory drift to compensate any change in mechanical angular momentum, resulting in horizontal motion if runaways are accelerated or decelerated. This horizontal drift is directional, as opposed to the diffusion-like behavior of stochastic scattering[22,23]. However, the result of Ref. 19 can not be directly applied to the aforementioned inward drift, due to the fact that the current during plateau regime is carried by runaway electrons themselves. Thus its crucial for us to go beyond test particle model and consider the runaway

orbit drift as an nonlinear process, so that any drift relative to the magnetic axis will result in further displacement of axis itself.

In this paper, the aforementioned inward drift is studied by considering the current carrying runaway electrons in an 2D equilibrium during runaway plateau regime. Those runaways are being decelerated by effective radiation drag as the original inductive accelerating field is greatly reduced during plateau[20]. It is found that the runaway current always move inward due to the requirement of canonical angular momentum conservation if their momentum is decreasing. It is also found that the eddy current and the vertical field are important in stabilizing this inward drift. In the absence of both, the runaways will not stop until it hit the first wall even for very small amount of momentum loss. A characteristic time scale is estimated by considering the synchrotron radiation and bremsstrahlung radiation drag, and the result is found to reasonably agree with experimental observations. This agreement indicates the inward drift motion we discuss here plays an important role in understanding runaway displacement during plateau regime.

The rest of the paper will be arranged as follows. In Section II, the transit orbit of runaway electrons will be given by seeking its constant canonical angular momentum of runaways. In Section III, we consider the displacement of runaway current center for any variation of parallel momentum. The zeroth order drift of runaway current will be given as a function of runaway momentum change for both ideally conducting wall case and no wall case. Further, a characteristic time scale of such drift will be estimated using effective radiation drag. In Section IV, a conclusion of the work will be given.

II. TRANSIT ORBIT OF RUNAWAY ELECTRONS

We consider a large aspect ratio toroidal system with major radius R, while R_0 is defined as major radius corresponding to the geometry center of the poloidal cross section of the system. For simplicity, we consider the first wall to be a rectangle toroid elongated along Z direction. Let the short side of the rectangle be $2a$, while the long side of it be $4a$. The inverse aspect ratio $\epsilon \equiv a/R_0$ is a small number. Four walls of the toroid are designated by numbers respectively.

A schematic plot of the system of interest is shown in Fig. 1 along with two coordinate

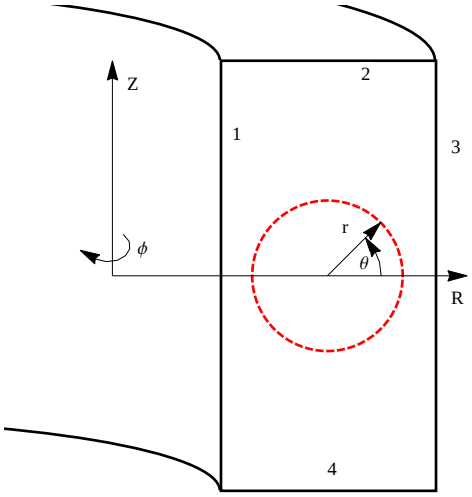

FIG. 1. A schematic plot for the cross section of the system of interest. The ideal wall is seen as a rectangle toroid as shown in the figure by the black solid lines. The red dashed circle represent the cross section of runaway torus on this RZ plane. The two coordinate system $(R, -\phi, Z)$ and (r, θ, ϕ) are also shown in the figure.

systems $(R, -\phi, Z)$ and (r, θ, ϕ). It should be noted that R_0 does not necessarily correspond to the runaway current center. Since we are primarily interested in the orbit drift of runaways, no velocity space instabilities will be discussed. Also, since the vertical stability of the runaway current is essentially a equilibrium problem which is a separate topic from what we are concerned here, it will not be treated in our consideration as well.

We will obtain the transit orbit of runaway electrons by seeking its constant canonical angular momentum surface. An easy way to see how this is done is to realize that the parallel momentum $p_\parallel$ is a near-constant across the transit orbit for runaway electrons, as the variation of perpendicular kinetic energy $\Delta(\mu B)$ is of $\mathcal{O}(\epsilon^3)$ comparing to $p_\parallel c$ if we assume $p_\perp/p_\parallel \sim \epsilon$. Thus the invariance of canonical angular momentum $p_\phi\left(p_\parallel, R, -\phi, Z\right)$ defines a 2D trajectory surface in configuration space for runaway electrons. A more rigorous consideration would write $p_\parallel$ as a function of Hamiltonian H and configuration space coordinates: $p_\parallel(H, R, -\phi, Z)$, then we have $p_\phi = p_\phi(H, R, -\phi, Z)$. The invariance of H and p_ϕ in time again defines the trajectory surface[21].

In our consideration, all of the runaways are assumed to be located on a torus with minor radius a_R, and with a single energy and pitch angle. While this is certainly not realistic, it serves to demonstrate the most fundamental physical idea. In reality, the runaway electrons

have a distribution both in configuration space and in velocity space, but the well known hollowed image of runaway radiation strongly suggest a hollowed spatial profile which peaks at certain minor radius[17,24,25], justifying our spatial assumption for the runaways as a zeroth order approximation. On the other hand, the single energy assumption is intended to mimic the "bump on tail" distribution of runaways in velocity space, as well as to greatly simplify the model. The effect of eddy current as a result of current center motion is taken into account by considering a simplified ideally conducting wall. This ideally conducting wall will stabilize current displacement, thus serving as a maximum stabilization scenario. In real tokamak, it's effect will be reduced by finite resistivity.

Since assuming all the runaways are of the same energy and pitch angle, its sufficient for us to write down the Lagrangian of a single runaway electron to describe dynamic of the whole runaway torus. We write down the relativistic guiding center Lagrangian for runaways as follows[19]:

$$L\left(\mathbf{x},\dot{\mathbf{x}},t\right)=\left[e\left(\mathbf{A}_R+\mathbf{A}_w+\mathbf{A}_d+\mathbf{A}_{ex}+\mathbf{A}_c\right)+p_{\parallel}\hat{b}\right]\cdot\dot{\mathbf{x}}-\gamma mc^2. \tag{1}$$

Here, e is the charge of electron, m is electron mass, c is the speed of light, $\hat{b}$ denotes the direction of magnetic field which is largely in toroidal direction due to the strong toroidal guiding field. γ is the relativistic factor:

$$\gamma=\sqrt{1+\frac{p_{\parallel}^2}{m^2c^2}+\frac{2\mu B}{mc^2}}. \tag{2}$$

B stand for the magnetic field, and the magnetic momentum is $\mu\equiv p_{\perp}^2/2mB$, while $p_{\parallel}$ and $p_{\perp}$ are the momentum parallel and perpendicular to the field line, respectively.

We now look at the contribution from vector potentials term by term, $\mathbf{A}_R$ is the vector potential generated by the runaway current, $\mathbf{A}_w$ is the vector potential corresponding to eddy current generated in a ideally conducting wall as a reaction to runaway current motion. Thus $\mathbf{A}_R+\mathbf{A}_w$ describe the total vector potential of a runaway current loop surrounded by the first wall. $\mathbf{A}_d$ represents the effective vector potential changed due to effective radiation drag, such that we have[5,7]

$$\mathbf{E}_d=-\frac{\partial\mathbf{A}_d}{\partial t}, \tag{3}$$

while the value of E_d is given by

$$\mathbf{E}_d=\mathbf{E}_{sd}+\mathbf{E}_{bd}, \tag{4}$$

$$E_{sd} = \frac{2}{3} r_e \frac{mc^2}{e} \left(\frac{\sqrt{\gamma^2 - 1}}{\gamma} \right)^3 \gamma^4 \left(\frac{1}{R_c^2} + \frac{\sin^4 \theta}{\rho_g^2} \right), \tag{5}$$

$$E_{bd} = \frac{4}{137} n_e \left(Z_{eff} + 1 \right) r_e^2 \frac{mc^2}{e} \gamma \left(\ln 2\gamma - \frac{1}{3} \right). \tag{6}$$

Here, E_{sd} and E_{bd} stand for the effective drag field from synchrotron radiation and bremsstrahlung radiation respectively. In the above equations, $r_e = e^2/4\pi\epsilon_0 mc^2$ is the classical electron radius, $\rho_g = p_\perp / eB_0$ is the electron gyro-radius, R_c is the major radius of runaway current center, $sin\theta = p_\perp / p$ is the pitch angle, n_e is the remnant plasma density after disruption and Z_{eff} is the effective charge of remnant plasma. Apart form those contributions, A_{ex} corresponds to an additional toroidal electric field which is generated by external coil and has the following form:

$$\mathbf{E}_{ex}(R) = -\frac{\partial \mathbf{A}_{ex}}{\partial t}, \tag{7}$$

$$\mathbf{E}_{ex} = E_{ex0} \frac{R_0}{R} \hat{\phi}. \tag{8}$$

We should point out that, since we are considering runaway electrons with high energy, the current carried by those electrons is just:

$$I_R = N_R e c. \tag{9}$$

Here, N_R is the total runaway population. Hence we know that the kinetic energy change of those electrons will only have minimal impact on the current itself, so that the inductive electric field from the change of poloidal magnetic flux is negligible. In a more realistic consideration, the distribution of runaways in velocity space has to be considered, and there may be small inductive field exist due to low energy runaways slowing down thus reducing the runaway current. However, those inductive field would be much smaller than the toroidal field at the beginning of current quench due to the much slower current decay rate. Last, there is an additional contribution $\mathbf{A}_c$ representing the constant magnetic field imposed by external coils, which include a toroidal field along ϕ direction and a vertical field along Z direction:

$$\mathbf{B}_c = \mathbf{B}_T + \mathbf{B}_Z, \tag{10}$$

$$\mathbf{B}_T = -\frac{B_{T0} R_0}{R} \hat{\phi}, \quad \mathbf{B}_Z = B_{Z0} \hat{z}. \tag{11}$$

So that $\mathbf{A}_c$ can be chosen to have the following form:

$$\mathbf{A}_c = \frac{1}{2}\ln\left(\frac{R}{R_0}\right)R_0 B_{T0}\hat{z} - \frac{R_0 B_{T0} z}{2R}\hat{R} + \frac{1}{2}B_{Z0}R\hat{\phi}. \tag{12}$$

Only the ϕ component of $\mathbf{A}_c$ will contribute to the trajectory of runaway electrons. The constant B_{Z0} is chosen so that at the beginning of the runaway plateau the runaway current center coincide with the geometry center of the system R_0.

Now the vector potential contribution from the runaway current itself will be write down explicitly. We assume *a priori* that the radial variation of runaway orbit along θ direction is of $\mathcal{O}(\epsilon a_R)$, so that the poloidal cross-section of runaway orbit can be approximated as a circle. Hence the magnetic field directly generated by the runaway current is axis-symmetric with regard to the runaway current center in the large aspect ratio limit. We will check the validity of this assumption *a posteriori*. This yields the following simple contribution:

$$\mathbf{B}_\theta = \frac{\mu_0 I_R}{2\pi r}\hat{\theta}, \tag{13}$$

$$\mathbf{A}_R = -\frac{\mu_0 I_R}{2\pi}\frac{R_0}{R}\left[\ln\left|\frac{r}{a}\right|K(r-a_R) + \ln\left|\frac{a_R}{a}\right|I(r-a_R)\right]\hat{\phi}, \tag{14}$$

$$K(x) = 1, \quad (x \geq 0); \quad K(x) = 0, \quad (x < 0); \quad I(x) = 1 - K(x). \tag{15}$$

Here, r is the minor radius of runaway electrons relative to the runaway current center. The step function K and I represent the fact that there is no current within the runaway torus, thus the runaway current contribution to the poloidal field is zero within the torus, and the vector potential have a simple R_0/R behavior. Further, the response from the ideally conducting wall will be treated by simple magnetic image method. We treat the movement d of runaway current I_R effectively as adding a pair of new current, one at the original position of the current and with value $-I_R$ which cancels the original current, the other at distance d and with value I_R which represents the moved current. The image currents corresponding to those two effective currents then represent the eddy current contribution to current center displacement. A schematic plot of this treatment is shown in Fig. 2.

This yields:

$$\mathbf{A}_w = \mathbf{A}_w^{(+)} + \mathbf{A}_w^{(-)}, \tag{16}$$

$$\mathbf{A}_w^{(+)} = \frac{\mu_0 I_R}{2\pi}\frac{R_0}{R}\left(\ln\left|\frac{r_1^{(+)}}{a}\right| + \ln\left|\frac{r_2^{(+)}}{a}\right| + \ln\left|\frac{r_3^{(+)}}{a}\right| + \ln\left|\frac{r_4^{(+)}}{a}\right|\right)\hat{\phi}, \tag{17}$$

$$\mathbf{A}_w^{(-)} = -\frac{\mu_0 I_R}{2\pi}\frac{R_0}{R}\left(\ln\left|\frac{r_1^{(-)}}{a}\right| + \ln\left|\frac{r_2^{(-)}}{a}\right| + \ln\left|\frac{r_3^{(-)}}{a}\right| + \ln\left|\frac{r_4^{(-)}}{a}\right|\right)\hat{\phi}. \tag{18}$$

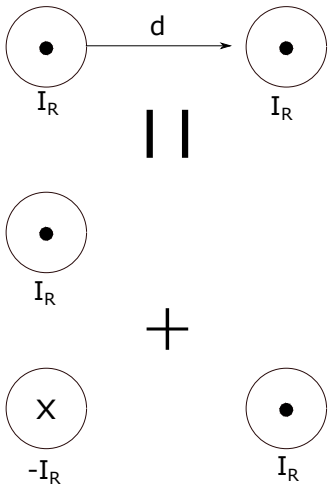

FIG. 2. A schematic plot for the treatment of current center displacement. The displaced current is effectively represented by adding two new current with value $-I_R$ and I_R respectively.

Here, $r_i^{(\pm)}$ represents the distance between runaway and the positive and negative image current centers generated by corresponding wall as designated in Fig. 1 respectively. For leading order contribution, it would be well enough for us to just take the four pairs of "primary" image currents directly corresponds to the current center displacement.

Finally, using above equations, Eq. 1 can be rewritten as follows:

$$L = p_r\dot{r} + p_\theta\dot{\theta} + p_\phi\dot{\phi} - H, \tag{19}$$

$$p_r = \frac{1}{2}e\ln\left(\frac{R}{R_0}\right)R_0B_0\sin\theta - e\frac{R_0B_0z}{2R}\cos\theta, \tag{20}$$

$$p_\theta = \frac{1}{2}e\ln\left(\frac{R}{R_0}\right)R_0B_0r\cos\theta - e\frac{R_0B_0rz}{2R}\sin\theta + (p + eA_d)\,r\sin\alpha, \tag{21}$$

$$p_\phi = \left[e\left(A_R + A_w + A_{ex} + \frac{1}{2}B_{Z0}R\right) + \left(p_\parallel + eA_d\right)\cos\alpha\right]R, \tag{22}$$

$$H = mc^2\sqrt{1 + \frac{p_\parallel^2}{m^2c^2} + \frac{2\mu B}{mc^2}}. \tag{23}$$

Here, α is defined as $\tan\alpha = B_\theta/B_T$, so that $\cos\alpha \sim 1$ for a large aspect ratio torus, and it can be approximately seen as a constant. It can be seen from Eq. 19 that there is no explicit dependence on ϕ in the Lagrangian, so that:

$$\frac{\partial L}{\partial\phi} = \frac{d}{dt}\frac{\partial L}{\partial\dot{\phi}} = \frac{d}{dt}p_\phi = 0. \tag{24}$$

That is, the symmetry of the system demands the canonical angular momentum of runaway electron to be a invariant in time. This invariant will define the surface of runaway orbit in configuration space.

Due to the symmetry along ϕ direction, this system is essentially 2D. It would be convenience for us to express the 2D poloidal plane in terms of Cartesian coordinates for the purpose of studying runaway orbit projection in this plane. We choose x to coincide with R, and y to coincide with Z. $x = 0$ corresponds to $R = R_0$, and $y = 0$ corresponds to $Z = 0$. Hence the r and $r_i^{(\pm)}$ variables in Eq. 14 and Eq. 16 can be expressed as:

$$r = \sqrt{(x-d)^2 + y^2}, \tag{25}$$

$$r_1^{(+)} = \sqrt{[x + (2a+d)]^2 + y^2}, \quad r_2^{(+)} = \sqrt{(x-d)^2 + (y-4a)^2}, \tag{26}$$

$$r_3^{(+)} = \sqrt{[x - (2a-d)]^2 + y^2}, \quad r_4^{(+)} = \sqrt{(x-d)^2 + (y+4a)^2}, \tag{27}$$

$$r_1^{(-)} = \sqrt{(x+2a)^2 + y^2}, \quad r_2^{(-)} = \sqrt{x^2 + (y-4a)^2}, \tag{28}$$

$$r_3^{(-)} = \sqrt{(x-2a)^2 + y^2}, \quad r_4^{(-)} = \sqrt{x^2 + (y+4a)^2}. \tag{29}$$

Here, $d \equiv R_c - R_0$ is the displacement of runaway current center relative to the geometric center of the system. Substituting Eq. 25 into Eq. 14 and Eq. 16, we then can seek the constant canonical angular momentum surface for runaways with a given momentum $p_\parallel$ by simply solving Eq. 22. This surface defines the runaway orbit in the magnetic field considered in our model. In this section, we will consider the displaced runaway orbit for changing parallel momentum as a sequence of stationary trajectory surfaces with time dependent terms dropped, each surface corresponds to a different parallel momentum and a different displacement. Direct impression of runaway orbit drift with respect to a given change in parallel momentum can then be obtained by comparing the original runaway orbit at the beginning of plateau with the decelerated one, as shown in Fig. 3 and Fig. 4 respectively.

The runaway current I_R acts as a given parameter and does not change in time. The radius of runaway torus is $a_R = 0.4a$. Further, the variation of $p_\parallel$ due to the inhomogeneity of magnetic field is negligible as $\gamma m_e c^2 \gg \mu B$.

In Fig. 3, the runaway orbit at the beginning of runaway plateau is shown. The runaway electron parallel momentum is set to be $p_{\parallel 0} = 2e\frac{\mu_0 I_R}{2\pi}\frac{R_0}{a}$, the constant vertical field is chosen as $B_{Z0} = -p_{\parallel 0}/eR_0$ so that the runaway current center will be at R_0. For runaway current on the order of $I_R \sim 0.1$ MA, the aforementioned choice of parallel momentum corresponds

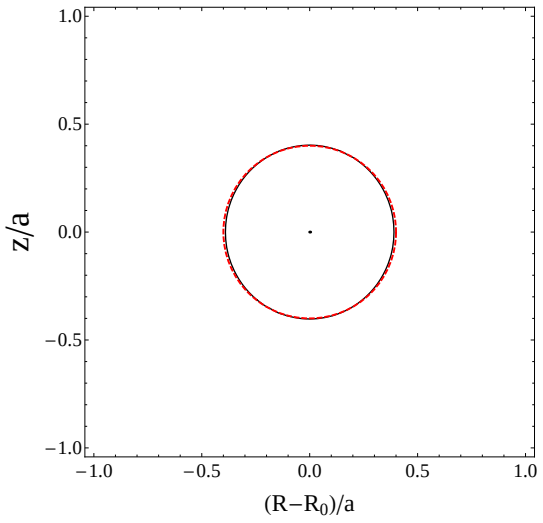

(a)

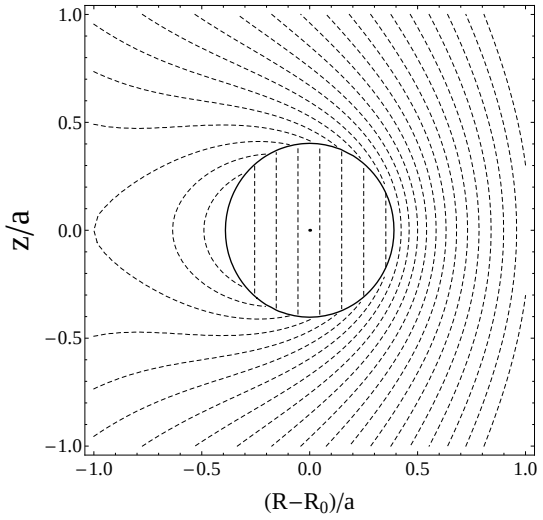

(b)

FIG. 3. The runaway electron orbit cross-section in the poloidal plane at the beginning of runaway plateau with relativistic factor $\gamma = 100$ and $I_R \sim 0.1$ MA. (a) The comparison between runaway orbit with current center at R_0 and a circle with minor radius $0.4a$. The black solid line represents the runaway orbit, and the red dashed line the analytical circle. (b) The runaway orbit in the background of total vector potential contour, which is represented by black dashed lines. The black dot in both figures denotes the position of runaway current center.

to a relativistic factor $\gamma = 100$. The inverse aspect ratio is chosen as $\epsilon = 0.2$. The runaway orbit is compared with a analytical circle with minor radius being $0.4a$ in Fig. 3 (a). In Fig. 3 (b), the orbit is put in the background of vector potential contour. The sudden change in the field behavior within the runaway torus is due to the step functions in Eq. 14, and will

not affect the runaway orbit in any way. Then we consider the case when the runaways have decelerated due to radiation drag. The relativistic factor is now $\gamma \simeq 68$, the displacement is found by calculating the constant p_ϕ contour iteratively so that the geometric center of orbit matches the current center position $R_0 + d$. The comparison between the orbit and a analytical circle with minor radius $0.4a$ is also shown in Fig. 4, as well as the total vector potential contour.

The most important feature obtained from this comparison is that runaway electrons will drift inward as long as they are decelerating, which will contribute to the inward runaway current drift observed in runaway plateau regime. The detailed dynamic of this inward drift will be discussed in Section III. Also, it can be seen that the deviation of runaway transit orbit from circle is less than $\mathcal{O}(\epsilon)$ comparing to a_R, justifying our assumption that the runaway orbit cross-section can be approximated as a circle even with substantial displacement.

III. INWARD DRIFT OF RUNAWAY ELECTRON TRANSIT ORBIT

The runaway orbit for a given $p_\parallel$ is demonstrated in Section II by iteratively seeking the constant p_ϕ surface. The explicit time dependence of this orbit is dropped. However, we are also interested in the dynamic of runaway orbit drift which is more relevant to the control of current displacement. That is, we wish to know analytically how much the displacement would be for a given change in runaway momentum $\Delta p_\parallel$. The time scale of this displacement is also of interest.

This dynamic can be get by considering the energy equation for runaways along with the invariance of canonical angular momentum. We write down the leading order change of runaway electron energy for one time period as[19]:

$$\Delta\left(\gamma m_e c^2\right) \simeq e\left(E_{ex0} + E_d\right) R_0 \dot{\phi}^{(0)} \Delta t, \tag{30}$$

where

$$\dot{\phi}^{(0)} = \frac{p_\parallel}{\gamma R_0 m_e}. \tag{31}$$

Here, Δt is a small time period, and any other Δf denotes the change of quantity f with regard to the unperturbed quantity. Most notably, we take $x = R - R_0$ as the relative major radial position of an arbitrary point on the transit orbit surface by the time t, then Δx

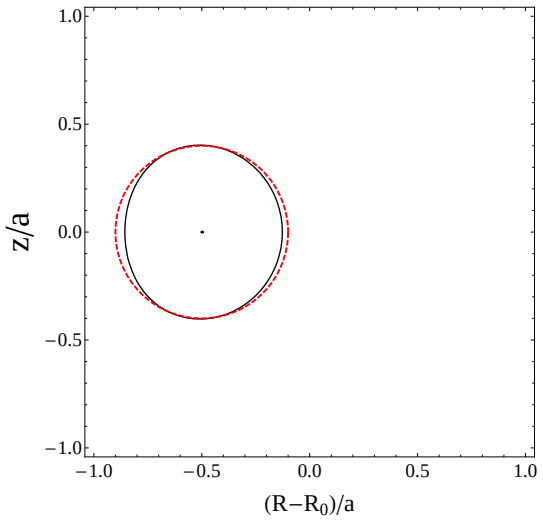

(a)

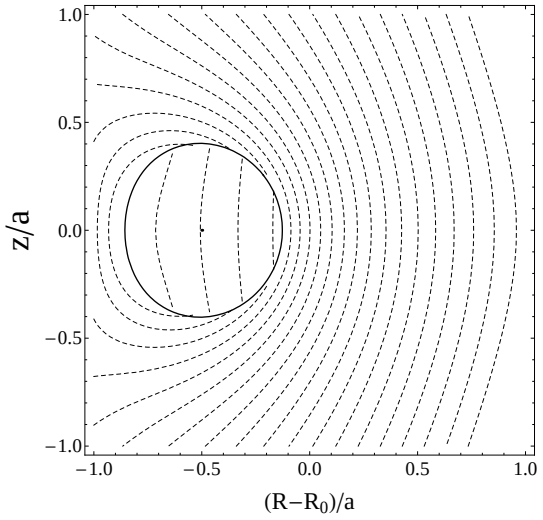

(b)

FIG. 4. The runaway electron orbit cross-section in the poloidal plane when current center displacement is $d = -0.5a$, corresponding $\gamma \simeq 68$ with the same I_R. (a) The comparison between runaway orbit with current center at R_0 and a circle with minor radius $0.4a$. The black solid line represents the runaway orbit, and the red dashed line the analytical circle. (b) The runaway orbit in the background of total vector potential contour, which is represented by black dashed lines. The black dot in both figures denotes the position of runaway current center.

would be the change of x for a time period Δt. A schematic plot for d, x, Δd and Δx is shown in Fig. 5. Hence we can write the change of parallel momentum for one time period

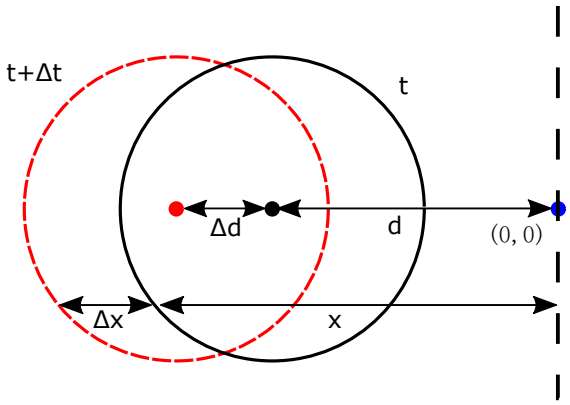

FIG. 5. A schematic plot for the runaway transit orbit at time t and $t+\Delta t$, with current center displacement d and $d+\Delta d$ respectively. The relative major radial position x for a arbitrary point on the transit orbit surface, and its displacement Δx after Δt is also shown on the plot.

up to $\mathcal{O}(\epsilon)$ as:

$$\Delta p_{\parallel} = e\left(E_{ex0}+E_d\right)\Delta t + \frac{m_e \mu B_{T0}\Delta x}{p_{\parallel}R_0}. \tag{32}$$

Meanwhile, the variation of $p_\phi = const$ provides the following relation for a given change in runaway parallel momentum $\Delta p_{\parallel}$:

$$e\Delta\left[\left(A_R+A_w\right)R\right] + eB_{Z0}R\Delta x - e\left(E_{ex0}+E_d\right)R_0\Delta t + \Delta p_{\parallel}R + p_{\parallel}\Delta x = 0. \tag{33}$$

Combining the evolution of runaway energy and invariance of its canonical angular momentum will then yield the dynamic of runaway current center displacement. It would be convenient to discuss the two extreme case where the time scale of runaway displacement is much shorter than the resistive time scale of the wall, and, conversely, the displacement time scale is much longer than the resistive time scale. In the former case, the eddy current from wall plays a crucial role in stabilizing the displacement of current center. In the latter case, this role will be undertaken by the constant vertical magnetic field.

A. Runaway drift dynamic with ideally conducting wall

Here, we consider the case where the time scale of runaway displacement is much shorter than the resistive time of the wall. Thus the wall can be seen as ideally conducting as studied in Section II.

Since we are considering the scenario where current is carried by runaway electrons themselves, the displacement of current center d also changes along with the position of runaways x. We have the following relation upon taking the circular cross-section approximation of runaway torus:

$$\Delta d \simeq \Delta x. \tag{34}$$

Hence we can proceed to write down the variation of runaway contribution:

$$e\Delta\left(A_R R\right) = -e\frac{\mu_0 I_R R_0}{2\pi}\frac{\Delta r}{a_R} = -e\frac{\mu_0 I_R R_0}{2\pi}\frac{\left(x-d\right)\left(\Delta x-\Delta d\right)}{a_R^2} \simeq 0. \tag{35}$$

It can be seen that the contribution from runaway current itself vanishes. This has the important implication that, unlike the poloidal field generated by background plasma current in Ref. 19, the poloidal field directly generated by runaway torus will not stabilize the orbit drift. That is, if there is not wall current or external vertical field, the orbital drift of runaway electron will not stop until it hit the first wall.

The contribution from eddy current is:

$$\Delta\left(A_w^{(\pm)} R\right) = \pm\frac{\mu_0 I_R R_0}{2\pi}\left[\frac{\Delta r_1^{(\pm)}}{r_1^{(\pm)}} + \frac{\Delta r_2^{(\pm)}}{r_2^{(\pm)}} + \frac{\Delta r_3^{(\pm)}}{r_3^{(\pm)}} + \frac{\Delta r_4^{(\pm)}}{r_4^{(\pm)}}\right]. \tag{36}$$

The variation of $A_w^{(-)}$ is straight forward as the position of image current has no dependence on the actual current displacement d. Hence, we have:

$$\frac{\Delta r_1^{(-)}}{r_1^{(-)}} = \frac{\left(x+2a\right)}{\left(x+2a\right)^2+y^2}\Delta x, \quad \frac{\Delta r_2^{(-)}}{r_2^{(-)}} = \frac{x}{x^2+\left(y-4a\right)^2}\Delta x, \tag{37}$$

$$\frac{\Delta r_3^{(-)}}{r_3^{(-)}} = \frac{\left(x-2a\right)}{\left(x-2a\right)^2+y^2}\Delta x, \quad \frac{\Delta r_4^{(-)}}{r_4^{(-)}} = \frac{x}{x^2+\left(y+4a\right)^2}\Delta x. \tag{38}$$

One the other hand, the displacement of current center d must be considered for $A_w^{(+)}$, so that we have:

$$\frac{\Delta r_1^{(+)}}{r_1^{(+)}} = \frac{2\left[x-d+2\left(a+d\right)\right]}{\left[\left(x-d\right)+2\left(a+d\right)\right]^2+a_R^2-\left(x-d\right)^2}\Delta x, \quad \frac{\Delta r_2^{(+)}}{r_2^{(+)}} = 0, \tag{39}$$

$$\frac{\Delta r_3^{(+)}}{r_3^{(+)}} = \frac{2\left[x-d-2\left(a-d\right)\right]}{\left[\left(x-d\right)-2\left(a-d\right)\right]^2+a_R^2-\left(x-d\right)^2}\Delta x, \quad \frac{\Delta r_4^{(+)}}{r_4^{(+)}} = 0. \tag{40}$$

Recall that we can approximate the poloidal cross-section of runaway orbit as a circle, so that $y \simeq \sqrt{a_R^2-\left(x-d\right)^2}$. Also recall that a_R and a are all constant. Hence we can write:

$$\Lambda\left(x,d\right) \equiv \sum_i \pm\frac{\Delta r_i^{(\pm)}}{r_i^{(\pm)}}\left(\Delta x\right)^{-1}. \tag{41}$$

This new function Λ is a function of the major radial position of runaways x and the current center displacement d. In the limit of $|x-d|$ being small, Λ reduce to the zeroth order approximation $\Lambda^{(0)}(d)$ which is a function of d alone.

Now we now can simplify Eq. 33 into:

$$e\frac{\mu_0 I_R R_0}{2\pi}\Lambda(x,d)\,\Delta x + eB_{Z0}R\Delta x + e\left(E_{ex0}+E_d\right)x\Delta t + \frac{m_e\mu B_{T0}\Delta x}{p_\parallel R_0}R + p_\parallel\Delta x = 0. \tag{42}$$

Recall that $B_{Z0} = -p_{\parallel 0}/eR_0$ is required for the current center being at R_0 for $t=0$, we have:

$$e\frac{\mu_0 I_R R_0}{2\pi}\Lambda(x,d)\,\Delta x - \left(p_{\parallel 0}-p_\parallel\right)\Delta x - p_{\parallel 0}\frac{x}{R_0}\Delta x + \frac{m_e\mu B_{T0}}{p_\parallel^2}\frac{R}{R_0}p_\parallel\Delta x = -e\left(E_{ex0}+E_d\right)x\Delta t. \tag{43}$$

Simple observation by iteratively seeking the constant p_ϕ surface indicates that $\left|p_{\parallel 0}-p_\parallel\right| \sim \left|e\frac{\mu_0 I_R R_0}{2\pi}\Lambda(x,d)\right|$ for significant displacement of current center. Based on this estimation, order analysis assuming $p_{\parallel 0}\sim\mathcal{O}(1)$ then yield the following ordering:

$$e\frac{\mu_0 I_R R_0}{2\pi}\Lambda(x,d) \sim \left(p_{\parallel 0}-p_\parallel\right) \sim \mathcal{O}\left(\left|\frac{d}{a}\right|\right), \tag{44}$$

$$p_{\parallel 0}\frac{x}{R_0} \sim \mathcal{O}\left(\epsilon\left|\frac{d}{a}\right|\right), \tag{45}$$

$$\frac{m_e\mu B_{T0}}{p_\parallel^2}\frac{R}{R_0}p_\parallel \sim \mathcal{O}\left(\epsilon^2\right). \tag{46}$$

Hence, to the lowest order, we have:

$$e\frac{\mu_0 I_R R_0}{2\pi}\Lambda(x,d)\,\Delta x - \left(p_{\parallel 0}-p_\parallel\right)\Delta x = -e\left(E_{ex0}+E_d\right)x\Delta t. \tag{47}$$

Due to the complicity of $\Lambda(x,d)$ and the contribution from parallel momentum term, it is hard to write a comprehensive expression of the drift rate $\Delta x/\Delta t$ analytically. However, Eq. 32 and Eq. 47 can be solved as two first order ODE if we only consider the dominant contributions. We define the following normalized parallel momentum and a new time scale for momentum change:

$$\bar{p}_\parallel \equiv \left(e\frac{\mu_0 I_R}{2\pi}\frac{R_0}{a}\right)^{-1} p_\parallel, \tag{48}$$

$$\tau_p^{-1} \equiv \left(E_{ex0}+E_d\right)\left(\frac{\mu_0 I_R R_0}{2\pi a}\right)^{-1}. \tag{49}$$

So that we can write down the evolution of current center displacement by taking the zeroth order approximation:

$$\frac{\Delta x}{\Delta t} \simeq \frac{\Delta d}{\Delta t} = \tau_p^{-1} \left[\left(\bar{p}_{\|0} - \bar{p}_{\|} \right) - a\Lambda^{(0)}\left(d\right) \right]^{-1} d, \tag{50}$$

$$\frac{\Delta \bar{p}_{\|}}{\Delta t} = \tau_p^{-1}. \tag{51}$$

It is noteworthy that, in a retrospective point of view, the runaway displacement does not really depends on the time history of momentum change. Combining Eq. 50 and Eq. 51, we can get a simple first order ODE regarding runaway displacement d and parallel momentum:

$$\frac{\Delta d}{\Delta \bar{p}_{\|}} = \left[\left(\bar{p}_{\|0} - \bar{p}_{\|} \right) - a\Lambda^{(0)}\left(d\right) \right]^{-1} d. \tag{52}$$

Thus runaway displacement is purely a function of the change in parallel momentum and is virtually independent of detailed models regarding how the parallel momentum is changed, which only affect the time scale of said displacement. In a more realistic model with finite resistive wall, however, the momentum change rate may be important if it is comparable with the inverse resistive time of the wall.

Eq. 52 can be solved by simple 4th order Runge-Kutta method[26] to get the relation between $p_{\|}$ and d. Using this relationship, the velocity of runaway drift motion can be obtained using Eq. 50. For simplicity, we consider a special case where τ_p^{-1} is a constant, so that the drift velocity $\Delta d/\Delta t$ can be simply plotted as a function of d. An example case with runaway torus radius $a_R = 0.3$ is presented in Fig. 7. Both the velocity of current center drift $\Delta x/\Delta t$ and the parallel momentum $p_{\|}$ as functions of current center displacement d is shown. It can be seen that for significant displacement of current center $p_{\|0} - p_{\|} \sim p_{\|0}$, confirming our previous ordering analysis. It can also be seen that the drift velocity is on the order of a/τ_p when the current center is away from the ideally conducting wall. When closing to the wall, its motion is stabilized by the strong magnetic field provided by the wall current.

To estimate the time scale of this drift motion, especially the motion far away from wall, we now estimate the magnitude of τ_p. For our case considered here, $\frac{\mu_0 I_R R_0}{2\pi a} = 1 \times 10^{-1} V \cdot s/m$, and the effective drag field can be estimated using Eq. 3 - Eq. 6 with $\gamma \sim 100$, $B_{T0} \sim 3$T and $p_{\perp}/p_{\|} \sim \epsilon$. The resulting effective drag field is on the order of 1.19 V/m. Hence the characteristic time scale of runaway orbit drift is $\tau_d \sim \tau_p \simeq 8.4 \times 10^{-2}$s. This time scale

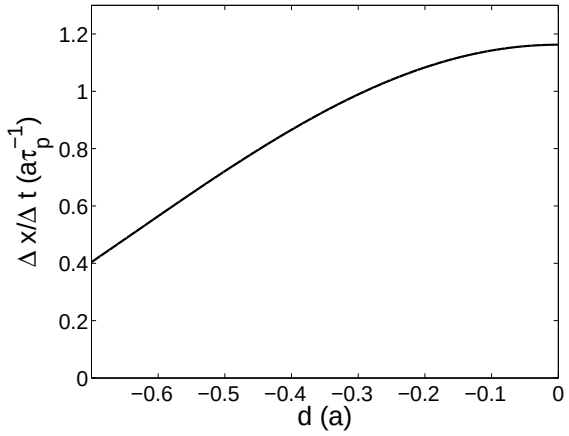

(a)

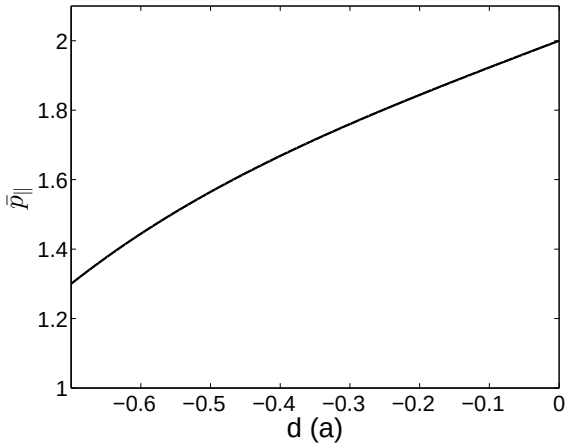

(b)

FIG. 6. (a) The velocity of current center drift as a function of current displacement. (b) The variation of parallel momentum as a function of current center displacement.

reasonably agree with experimental observation, where the current center moves one third of the minor radius in 25ms[17]. This corresponds to a time scale about 8.75×10^{-2}s.

As a further note, the displacement of the left and right extreme points of the runaway torus can be studied by considering $\Lambda(x, d)$ rather than $\Lambda^{(0)}(d)$ in Eq. 50. The position of left and right extreme point of torus as functions of current center displacement are shown in Fig. 6. It can be seen that apart from the drift along with the current center, there are additional next order motion which tend to "squeeze" the cross-section of runaway orbit. This corresponds to the deformation of runaway cross-section seen in Fig. 4.

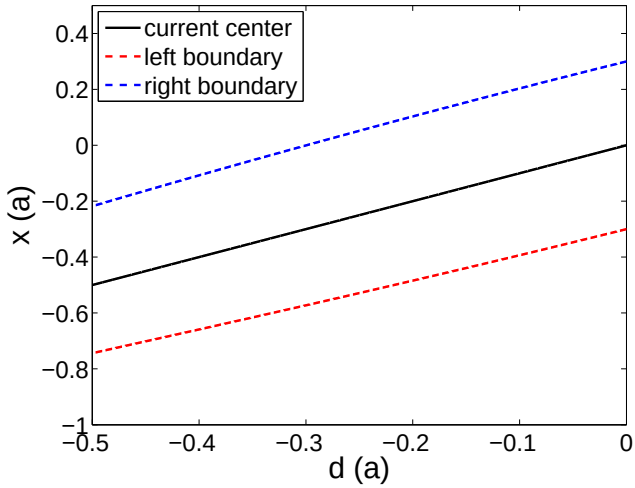

FIG. 7. The position of current center and both extreme points of the runaway torus as functions of the current center displacement. It can be seen that there is only minimal deformation of the circular even for significant displacement of current center.

B. Runaway drift dynamic with highly resistive wall

Another interesting scenario is the case where the time scale of current center drift is much longer than the resistive time scale of the wall. In this case, the wall can be seen as magnetically transparent. That is, there is no response from wall current to the change of magnetic field within the vessel.

Under this consideration, Eq. 43 becomes:

$$-p_{\|0}\frac{x}{R_0}\Delta x+\frac{m_e\mu B_{T0}}{p_\|^2}\frac{R}{R_0}p_\|\Delta x=-e\left(E_{ex0}+E_d\right)x\Delta t. \tag{53}$$

Following a similar ordering analysis carried out in the previous section, we have:

$$-p_{\|0}\frac{x}{R_0}\sim\mathcal{O}\left(\epsilon\left|\frac{d}{a}\right|\right), \tag{54}$$

$$\frac{m_e\mu B_{T0}}{p_\|^2}\frac{R}{R_0}p_\|\sim\mathcal{O}\left(\epsilon^2\right). \tag{55}$$

Hence the dominant contribution now is:

$$\bar{p}_{\|0}\frac{1}{R_0}\Delta x=\tau_p^{-1}\Delta t. \tag{56}$$

$$\Delta\bar{p}_\|=\tau_p^{-1}\Delta t. \tag{57}$$

The relationship between runaway displacement and parallel momentum change is then simply:

$$\frac{\Delta x}{\Delta \bar{p}_{\|}} = \frac{\Delta d}{\Delta \bar{p}_{\|}} = \frac{R_0}{\bar{p}_{\|0}}. \tag{58}$$

And the drift velocity of runaway electrons is also very simple:

$$\frac{\Delta x}{\Delta t} = \frac{\Delta d}{\Delta t} = \frac{e\left(E_{ex0} + E_d\right) R_0}{p_{\|0}}. \tag{59}$$

This result is essentially along the same line with the scenario studied bu Guan et al. in Ref. 19, as both cases concerns the drift of runaway electrons in a prescribed magnetic field. The only difference is that Guan et al. studied the outward drift of accelerating runaways in a constant poloidal field carried by plasma current, while here we are looking at the inward drift of decelerating runaways in a constant vertical field sustained by external coils.

The time scale of this drift motion can again be estimated by considering runaway electrons with $\gamma \sim 100$, $B \sim 3$T and $R_0 \sim 2$m. The effective drag field is again 1.19 V/m, as is in the previous section. The time scale for current center drifting across the vessel is then $\tau_d \sim 2.5 \times 10^{-2}$s. This times scale is of $\mathcal{O}(\epsilon)$ comparing to the time scale of the ideally conducting case. This is consistent with the fact that the LHS of Eq. 56 is of $\mathcal{O}(\epsilon)$ comparing to the LHS of Eq. 47.

IV. DISCUSSION AND CONCLUSION

The inward drift of runaway current center during runaway plateau is studied in this paper. This horizontal drift motion is required by the conservation of canonical angular momentum to balance any change of parallel mechanical momentum of runaway electrons. We are mainly interested in the plateau regime after disruption where most of the current is carried by runaway electrons themselves. In this consideration, for any drift of runaway electron relative to the field line, the current center itself will also drift. Since the magnetic field lines is generated by this runaway current, the resulting current center drift motion is essentially non-linear, as oppose to the linear drift motion of test particle runaways studied in previous works[19].

The runaway transit orbit surface is obtained by seeking the constant canonical angular momentum surface in a unperturbed 2D equilibrium. It is found that runaways will always

drift inward as long as they are losing momentum. The eddy current and external vertical field are found to play a crucial role in stabilizing this horizontal drift, without which the runaways will not stop until they hit the first wall even for small amount of momentum loss. The dynamic of this inward drift is analyzed by taking the variation of canonical angular momentum and electron energy, which yield a first order ODE describing the trajectory displacement for any given change in parallel momentum. The time scale of such displacement is estimated by using models of effective radiation drag. The time scale thus calculated reasonably agrees with experimental observation.

It is noteworthy that the horizontal drift we discussed here has drastically different physics with the force imbalance along major radius, which has been invoked when discussing the observed inward motion during plateau regime[16]. The fundamental physics here is the conservation of canonical angular momentum, which can not be recovered by simply considering the runaway current as an ordinary current carrying circuit. An easy way to see this is by considering a runaway torus in perfect force balance. We then consider a certain loss of parallel momentum, with minimal decrease in the velocity of runaways. The change in $\mathbf{J} \times \mathbf{B}$ force balance is negligible, but the runaways will still drift inward to preserve their canonical angular momentum. Hence our study here provided a new powerful mechanism which may play an important role in analyzing runaway motions during plateau regime.

Strong simplification has been made to ensure the runaway current drift we concerned here to be analytically tractable. In a more realistic consideration, various more complicated model such as finite distribution of runaways in phase space and the impact of finite resistive wall should be included. Tracking the evolution of thus more complicated model require numerical tools, and it is left for future works.

Acknowledgments

The authors thank C. Liu, X.-G. Wang and A. Bhattacharjee for fruitful discussion. This work is partially supported by National Magnetic Confinement Fusion Energy Research Project under Grant No. 2015GB111003, National Natural Science Foundation of China under Grant No. 1126114032, 11575185, 11575186 and 11305171, JSPS-NRF-NSFC A3 Foresight Program under Grant No. 11261140328, the China Scholarship Council and US DoE contract No. AC02-09-CH11466.

REFERENCES

[1]M. N. Rosenbluth and S. V. Putvinski, Nucl. Fusion **37** 1355 (1997);

[2]H. Smith, P. Helander, L.-G. Eriksson and T. Fülöp, Phys. Plasmas **12** 122505 (2005);

[3]H. Smith, P. Helander, L.-G. Eriksson, D. Anderson, M. Lisak and F. Andersson, Phys. Plasmas **13** 102502 (2006);

[4]T.C. Hender, J.C Wesley, J. Bialek, A. Bondeson, A.H. Boozer, R.J. Buttery, A. Garofalo, T.P Goodman, R.S. Granetz, Y. Gribov, O. Gruber, M. Gryaznevich, G. Giruzzi, S. Günter, N. Hayashi, P. Helander, C.C. Hegna, D.F. Howell, D.A. Humphreys, G.T.A. Huysmans, A.W. Hyatt, A. Isayama, S.C. Jardin, Y. Kawano, A. Kellman, C. Kessel, H.R. Koslowski, R.J. La Haye, E. Lazzaro, Y.Q. Liu, V. Lukash, J. Manickam, S. Medvedev, V. Mertens, S.V. Mirnov, Y. Nakamura, G. Navratil, M. Okabayashi, T. Ozeki, R. Paccagnella, G. Pautasso, F. Porcelli, V.D. Pustovitov, V. Riccardo, M. Sato, O. Sauter, M.J. Schaffer, M. Shimada, P. Sonato, E.J. Strait, M. Sugihara, M. Takechi, A.D. Turnbull, E. Westerhof, D.G. Whyte, R. Yoshino, H. Zohm and the ITPA MHD, Disruption and Magnetic Control Topical Group, Nucl. Fusion **47** S128 (2007);

[5]J. R. Martín-Solís, J. D. Alvarez, R.Sánchez and B. Espositp, Phys. Plasmas **5** 2370 (1998);

[6]F. Andersson, P. Helander and L.-G. Eriksson, Phys. Plasmas **8** 5221 (2001);

[7]M. Bakhtiari, G. J. Kramer and D. G. Whyte, Phys. Plasmas **12** 102503 (2005);

[8]E.M. Hollmann, M.E. Austin, J.A. Boedo, N.H. Brooks, N. Commaux, N.W. Eidietis, D.A. Humphreys, V.A. Izzo, A.N. James, T.C. Jernigan, A. Loarte, J. Martin-Solis, R.A. Moyer, J.M. Muñoz-Burgos, P.B. Parks, D.L. Rudakov, E.J. Strait, C. Tsui, M.A. Van Zeeland, J.C. Wesley and J.H. Yu, Nucl. Fusion **53** 083004 (2013);

[9]P. Aleynikov and B. N. Breizman, Phys. Rev. Lett. **114** 155001 (2005);

[10]J. Decker, E. Hirvijoki, O. Embreus, Y. Peysson, A. Stahl, I. Pusztai, T. Fülöp, arXiv:1503.03881v2 [physics.plasm-ph] (2015);

[11]E. Hirvijoki, I. Pusztai, J. Decker, O. Embréus, A. Stahl, T. Fülöp, arXiv:1502.03333v2 [physics.plasm-ph] (2015);

[12]G. Fussmann, Nucl. Fusion **19** 327 (1979);

[13]P. B. Parks, M. N. Rosenbluth and S. V. Putvinski, Phys. Plasmas **6** 2523 (1999);

[14]C. Liu, D. P. Brennan, A. H. Boozer and A. Bhattacharjee, arXiv:1509.04402v2 [physics.plasm-ph] (2015);

[15]R. D. Gill, B. Alper, M. de Baar, T. C. Hender, M. F. Johnson, V. Riccardo and contributors to the EFDA-JET Workprogramme, Nucl. Fusion **42** 1039 (2002);

[16]Eidietis, N. W. and Commaux, N. and Hollmann, E. M. and Humphreys, D. A. and Jernigan, T. C. and Moyer, R. A. and Strait, E. J. and VanZeeland, M. A. and Wesley, J. C. and Yu, J. H. Phys. Plasmas **19** 056109 (2012);

[17]Y. P. Zhang, Yi Liu, G. L. Yuan, M. Isobe, Z. Y. Chen, J. Cheng, X. Q. Ji, X. M. Song, J. W. Yang, and X. Y. Song, X. Li, W. Deng, Y. G. Li, Y. Xu, and T. F. Sun, and X. T. Ding, and L. W. Yan, and Q. W. Yang, and X. R. Duan, and Y. Liu, and HL-2A Team, Phys. Plasmas **19** 032510 (2012);

[18]S. V. Putvinski, P. Barabaschi, N. Fujisawa, N. Putvinskaya, M. N. Rosenbluth and J. Wesley, Plasma Phys. Control. Fusion **39** B157 (1997);

[19]X. Guan, H. Qin and N. J. Fisch, Phys. Plasmas **17** 092502 (2010);

[20]R. D. Gill, Nucl. Fusion **33** 1613 (1993);

[21]H. Qin, X. Guan and W. M. Tang, Phys. Plasmas **16** 042510 (2009);

[22]A. B. Rechester and M. N. Rosenbluth, Phys. Rev. Lett. **40** 38 (1978);

[23]H. E. Mynick and J. D. Strachan, Phys. Fluids **24** 695 (1981);

[24]V. V. Plyusnin, V.G. Kiptily, B. Bazylev, A.E. Shevelev, E.M. Khilkevitc, J. Mlynar, M. Lehnen, G. Arnoux, A. Huber, S. Jachmich, V. Riccardo, U. Kruezi, B.Alper, R.C. Pereira, A. Fernandes, C. Reux, P.C. de Vries, T.C. Hender and JET EFDA contributors, Proceeding of IAEA FEC2012, San Diego, USA (2012);

[25]R. J. Zhou, L. Q. Hu, E. Z. Li, M. Xu, G. Q. Zhong, L. Q. Xu, S. Y. Lin, J. Z. Zhang and the EAST Team, Plasma Phys. Control. Fusion **55** 055006 (2013);

[26]J. C. Butcher, "Numerical methods for ordinary differential equations". (John Wiley & Sons, New York, 2008), p. 93;